Appendix Table of Contents

Appendix Figure S1. Strategy for CRISPR-CAS9-mediated PTEN gene editing in Hela cells.

(**a**) Sequence analysis revealed a 21bp deletion in *PTEN* exon1 that leads to the appearance of a TAG stop codon (highlighted in red) immediately downstream of the AUU^{594} initiation codon of PTENβ. The initiation codon of PTENβ is highlighted in a red box.

(**b**) Sequence analysis revealed a C>T mutation in PTEN exon1 that leads to the appearance of a TAG stop codon (highlighted in red) at 48 bp upstream of the AUG^{1032} initiation codon of canonical PTEN. The initiation codon of canonical PTEN is highlighted in a red box.

(**c**) Sequence analysis revealed a frameshift that leads to the appearance of a TAG stop codon (highlighted in red) downstream of the AUG^{1032} initiation codon of canonical PTEN. The initiation codon of canonical PTEN is highlighted in a red box.

Appendix Figure S2. The immunoblots of exogenously expressed PTEN isoforms.

The plasmid used in Fig 2A lane 3 was introduced into Hela *PTEN*$^{-/-}$ cells. The transfected cells and Hela WT cells were harvested and the lysates were immunoblotted with a PTEN monoclonal antibody (Cell Signaling Technology, 138G6). GAPDH was used as a control. The white arrows indicate the protein bands of endogenous or exogenously expressed PTENε while the numbers in red demonstrate the relative grayscale of the corresponding protein.

Appendix Figure S3. The PTENε initiation site CUG^{816} is evolutionarily conserved.

Clustal-W alignment of the proximal sequence of Human PTENε initiation start site CUG^{816} with the

corresponding genomic sequence from Mus musculus, Minke Whale, Pan paniscus obtained from the Genebank. The conserved sequences are highlighted in yellow. The start site CUG^{816} in the N-terminal extended domain of PTENε is highlighted in the red box.

Appendix Figure S4. Validation of the subcellular localization of PTENε in the cell plasma membrane.

(**a**) Validation of single isoform expression of different C-GFP tagged PTEN variants shown in Fig 5A by immunoblotting. C-terminal GFP tagged PTEN, PTENα, PTENβ, and PTENε as indicated in Fig 5A were separately introduced into Hela *PTEN*$^{-/-}$ cells followed by immunoblotting with GFP (MBL) antibody. GAPDH was used as a control.

(**b**) Differing sets of PTEN and PTENε constructs. A TAG triplet was inserted in the C-terminus of PTEN and PTENε sequences in constructs indicated in Fig 5A to abolish the expression of the GFP tag.

(**c**) Subcellular localization of exogenous PTENε without any tag. Constructs in (**b**) were introduced into Hela *PTEN*$^{-/-}$ cells respectively. Twenty-four hours after transfection, cells were sequentially stained with anti-β-catenin, anti-PTEN monoclonal antibody (Cell Signaling Technology, 138G6), and DAPI, followed by imaging with confocal microscopy. The scale bars represent 8 μm.

Appendix Figure S5. Validation of the subcellular colocalization of PTENε with down-stream targets.

Colocalization of exogenous PTENε-GFP with FLAG-CDC42 or FLAG-ACTR2. Plasmids indicated

above were co-transfected into Hela *PTEN*$^{-/-}$ cells. Cells were stained with DAPI and a FLAG antibody (F3165), followed by imaging with confocal microscopy. The scale bars represent 5 μm.

Appendix Figure S6. PTENε, like canonical PTEN, acts as an antagonist of the PI3K pathway.

(**a**) C-terminal GFP tagged PTEN, PTENα, PTENβ, or PTENε was separately introduced into Hela *PTEN*$^{-/-}$ cells followed by immunoblotting with p-AKT(Ser473), AKT, GAPDH or GFP antibody.

(**b**) C-terminal HA-tagged wild type PTENε, PTENε with lipid phosphatase activity abolished (G201E, analogous to PTEN (G129E)), PTENε with protein phosphatase activity abolished (Y210L, analogous to PTEN (Y138L)) and PTENε with both lipid and protein phosphatase activity abolished (C196S, analogous to PTEN (C124S)) were introduced separately into Hela *PTEN*$^{-/-}$ cells, followed by immunoblotting with p-AKT (Ser473), AKT, GAPDH or HA antibody respectively.

Appendix Figure S7. Frequency of colony formation in Hela *PTEN*$^{-/-}$ cells and H4 human neuroglioma cells stably expressing PTENε or PTENε mutants.

(**a**) Hela *PTEN*$^{-/-}$ cells were infected with lentivirus expressing C-terminal HA-tagged PTENε or PTENε Y210L respectively and analyzed by western blot with a monoclonal PTEN antibody (Cell Signaling Technology, 138G6). GAPDH was used as a control.

(**b**) H4 human neuroglioma cells were infected with lentivirus expressing C-terminal HA-tagged PTENε or PTENε Y210L separately and analyzed by immunoblotting with a monoclonal PTEN antibody (Cell Signaling Technology, 138G6). GAPDH was used as a control.

(**c**) Colony formation assay was performed in Hela *PTEN*$^{-/-}$ cells stably expressing PTENε or PTENε

Y210L mutant. The number of colonies was counted by ImageJ software. Three representative fields of cells in each group were captured and calculated. Data are presented as the mean ± SD based on three independent experiments with at least three replicates and were analyzed with the unpaired t-test.

(**d**) Colony formation assay was performed in *PTEN* null H4 human neuroglioma cells stably expressing PTENε or PTENε Y210L mutant. Cells of each group (CTR, PTENε or PTENε Y210L) were seeded onto three wells of a 6 well plate, and three independent experiments were performed. Image J software was used to automatedly calculate the colony number of each well, and the mean value of cell colonies of each group in every independent experiment was used as input and analyzed by the two-tail unpaired t-test (Prism GraphPad software v8.0). Data are presented as the mean ± SD.

Appendix Figure S8. Strategy for adenine-base-editing-mediated depletion of endogenous PTENε and detection of potential off-targets in Hela cells.

(**a**) Sequence analysis revealed a heterozygous T>C mutation in PTENε alternative initiation site CTG^{816} that leads to the partial depletion of endogenous PTENε in Hela cells. The start site CUG^{816} in the N-terminal extended domain of PTENε is highlighted in the red box.

(**b**) Detection of potential off-targets in Hela $PTEN\varepsilon^{+/-}$ cells. The corresponding region of potential off-targets that may be misrecognized by ABE7.10 due to sgRNA mismatching was amplified through PCR and then sequenced. The results of sequencing were aligned with the correct genome sequences of relative genes by using Vector NTI software. The misrecognized region in the corresponding gene is highlighted in the red box.

Appendix Figure S9. A schematic representation of the PTEN family members.

A schematic representation of the PTEN family members. The proteins labeled with the question mark "?" stand for unidentified isoforms of PTEN that remain to be further verified.

Appendix Figure S10. Sequences supplemented in the UniProt database.

(**a, b**) The N-terminal extended PTEN sequence supplemented in the UniProt Human database (**a**) or the UniProt Mouse database (**b**) for a raw file searching by Proteome Discoverer. The most proximal N-terminal amino acids of PTENα, PTENβ, and PTENε are highlighted in blue, red, and green respectively.

Appendix Table S1. A list of antibodies used in this study

Appendix Table S2. Primers for constructing plasmids

Appendix Table S3. Primers for mutagenesis

Appendix Table S4. Primers for real-time PCR

Appendix Figures

Appendix Figure S1. Strategy for CRISPR-CAS9-mediated *PTEN* gene editing in Hela cells.

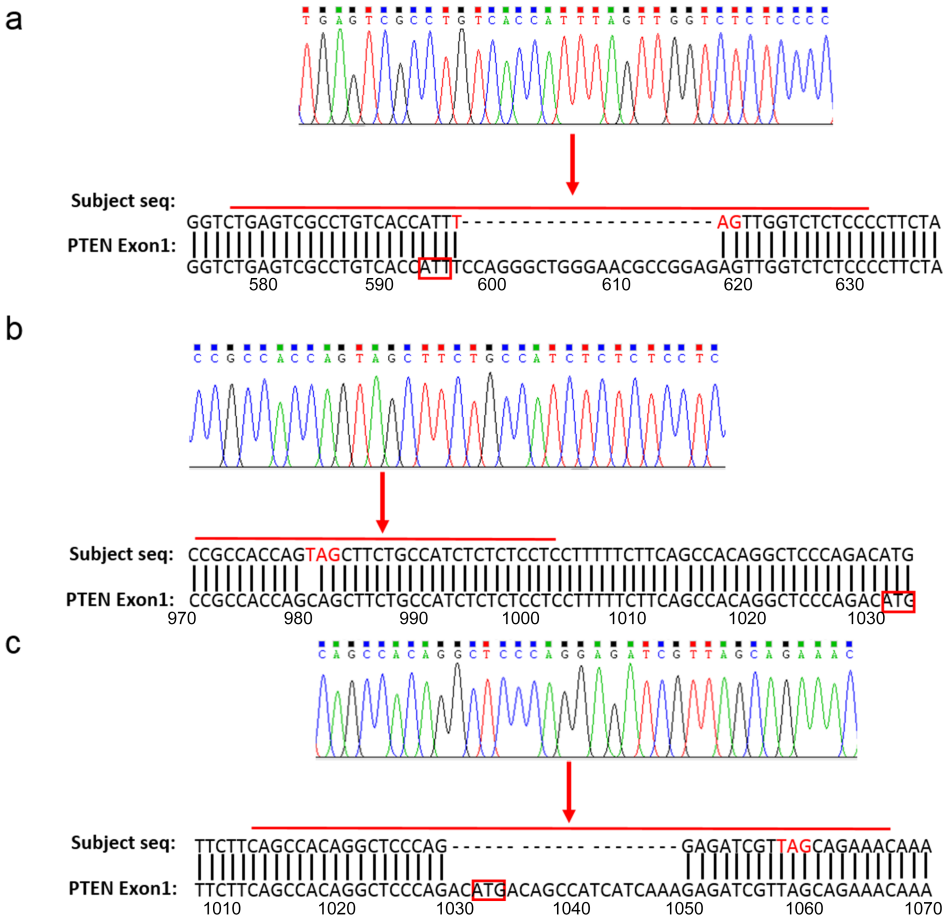

Appendix Figure S2. The immunoblots of exogenously expressed PTEN isoforms.

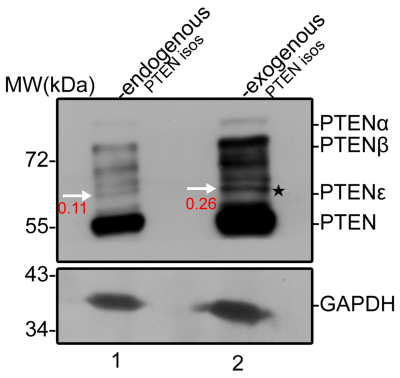

Appendix Figure S3. The PTENε initiation site CUG^{816} is evolutionarily conserved.

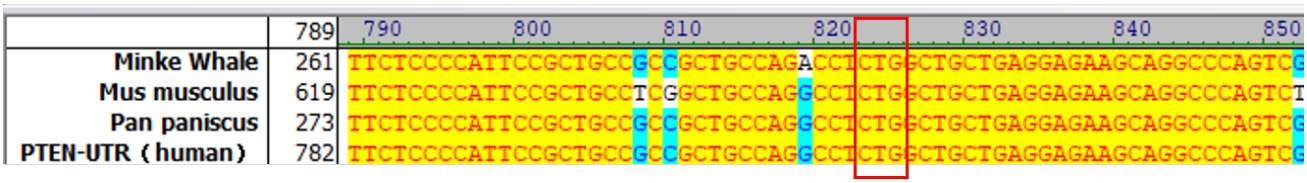

Appendix Figure S4. Validation of the subcellular localization of PTENε in the cell plasma membrane.

a

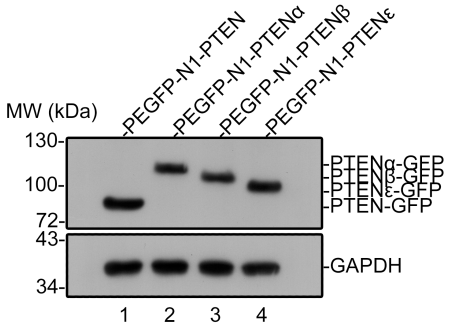

b

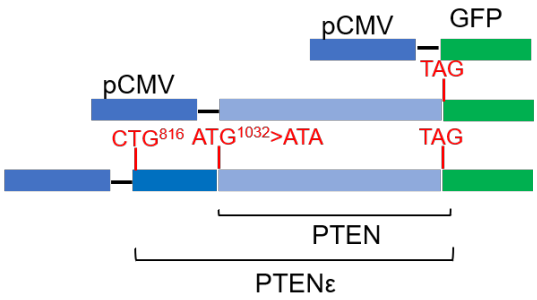

c

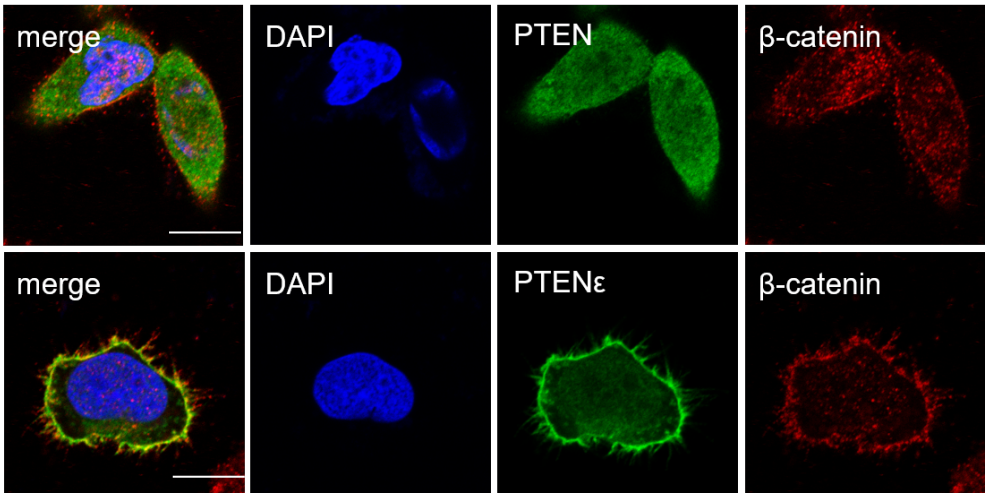

Appendix Figure S5. Validation of the subcellular colocalization of PTENε with down-stream targets.

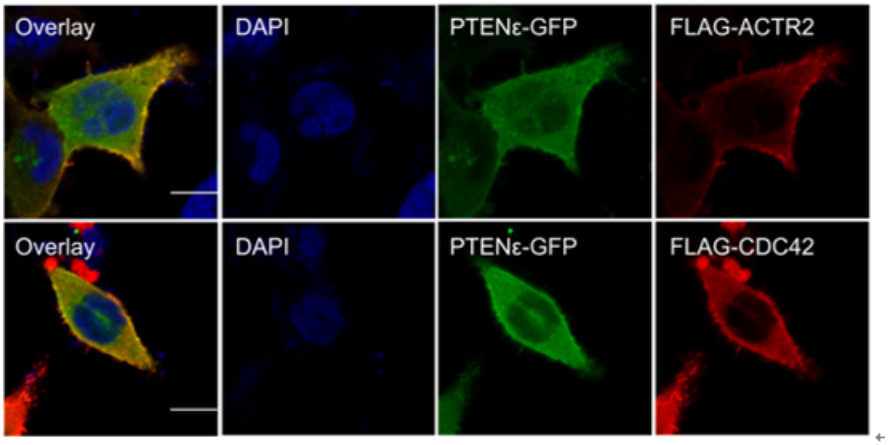

Appendix Figure S6. PTENε, like canonical PTEN, acts as an antagonist of the PI3K pathway.

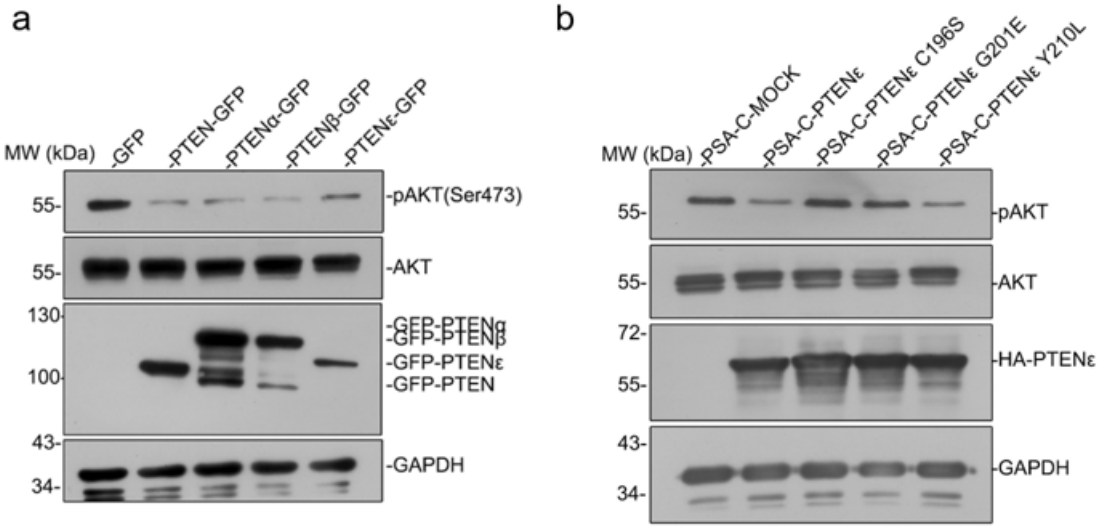

Appendix Figure S7. Frequency of colony formation in Hela *PTEN*$^{-/-}$ cells and H4 human neuroglioma cells stably expressing PTENε or PTENε mutants.

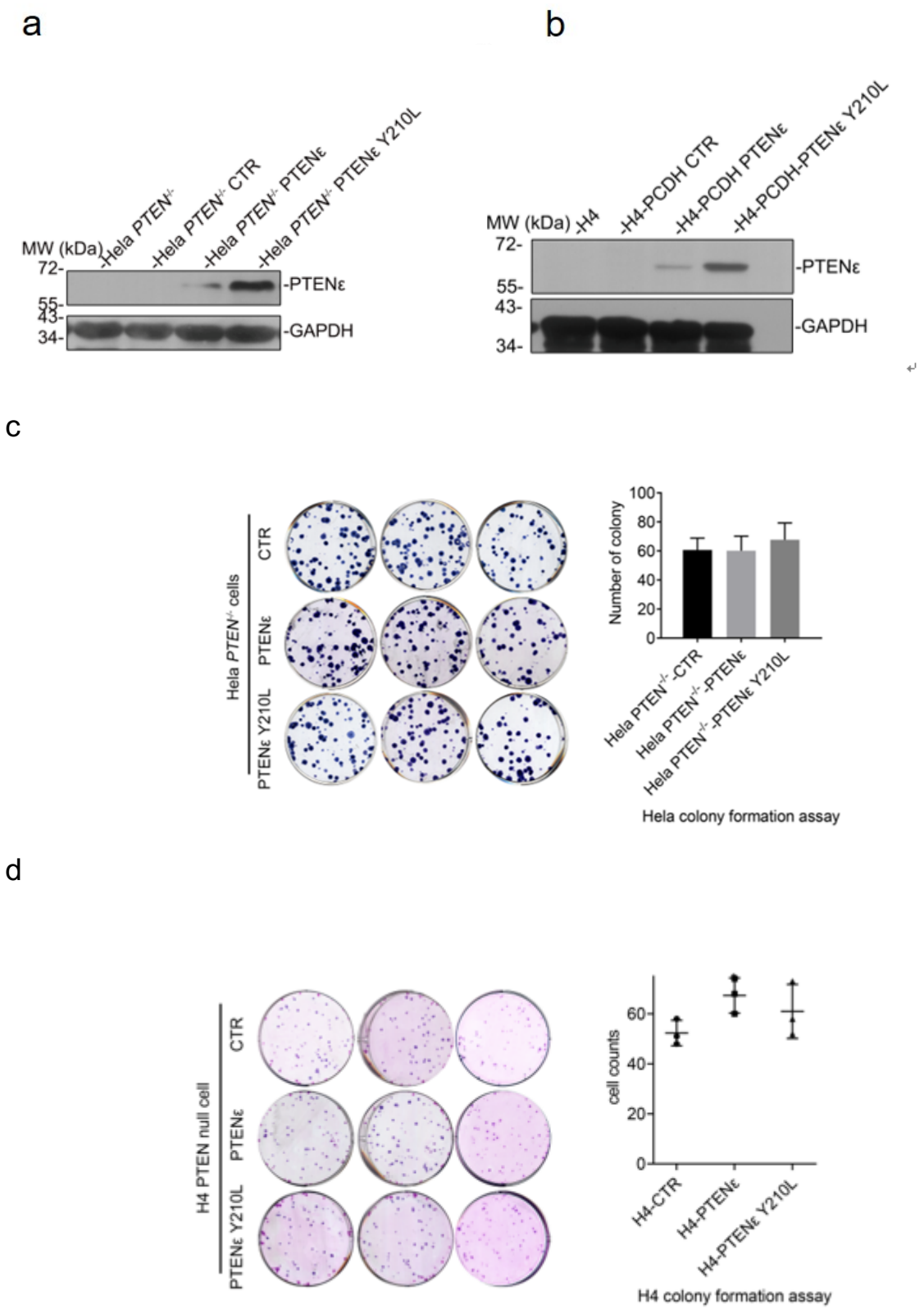

Appendix Figure S8. Strategy for adenine-base-editing-mediated depletion of endogenous PTENε and detection of potential off-targets in Hela cells.

a

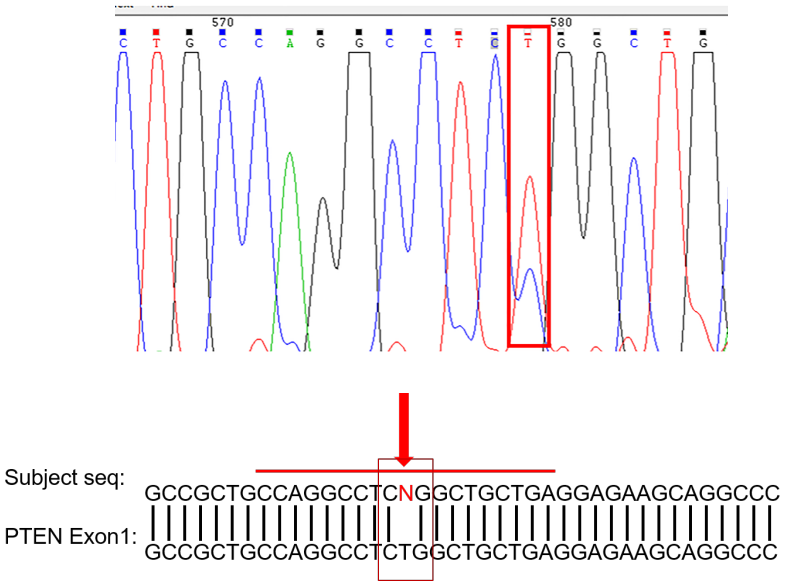

b

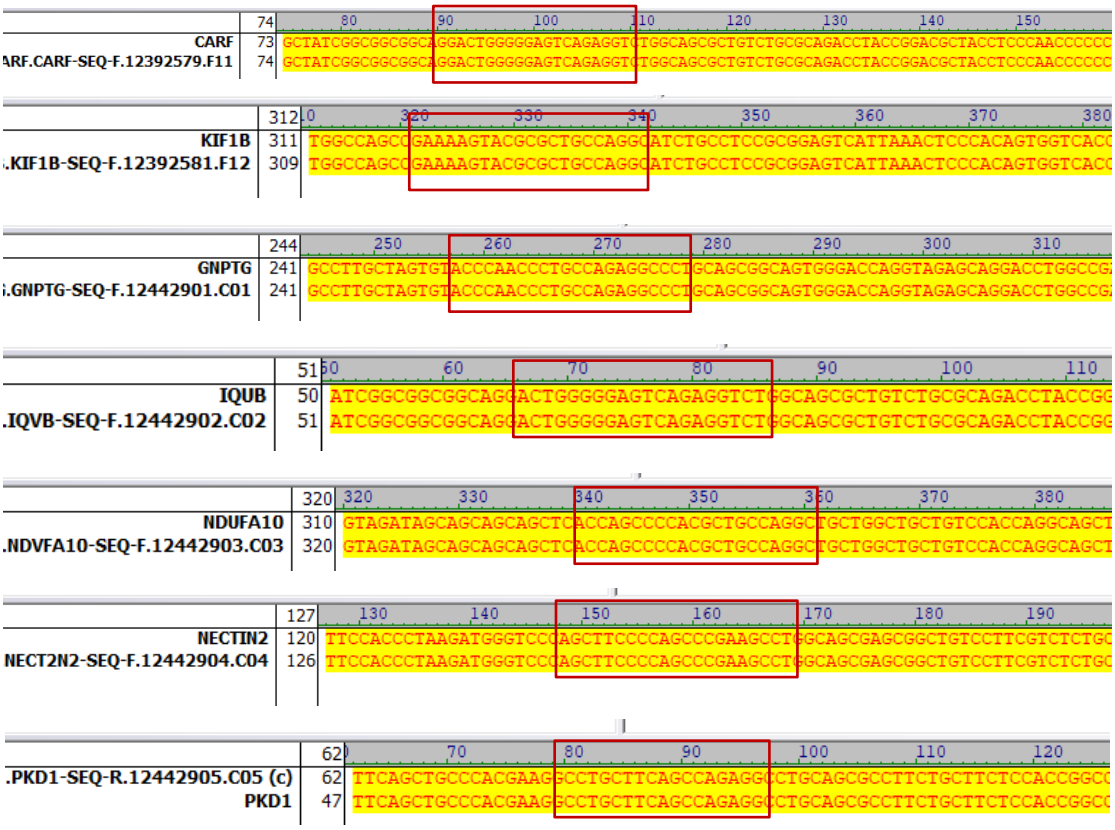

Appendix Figure S9. A schematic representation of the PTEN family members.

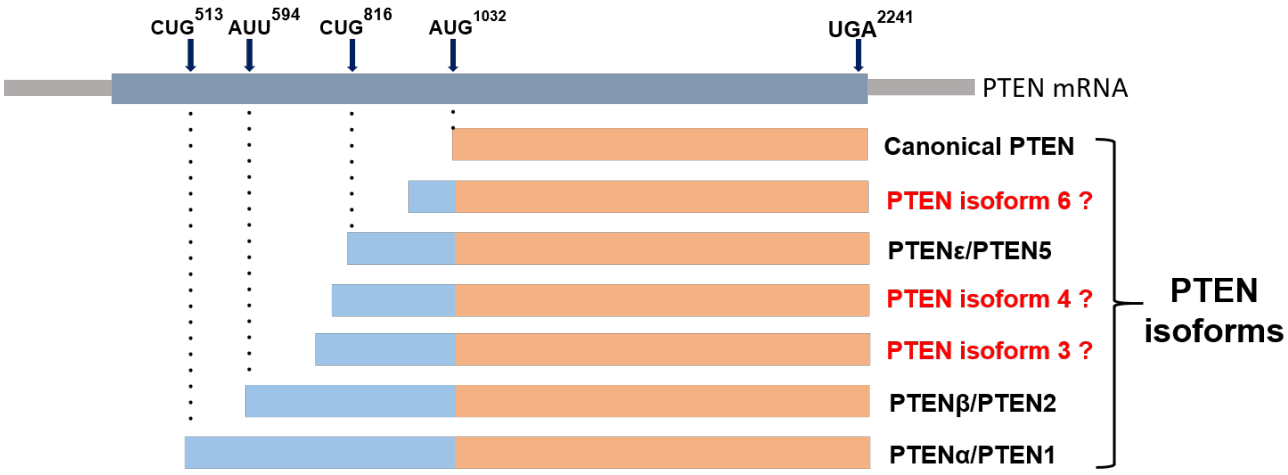

Appendix Figure S10. Sequences supplemented in the UniProt database.

Appendix Tables

Appendix Table S1. A list of antibodies used in this study

Species	Antigen	Clone #	Company (Cat#)	Dilution ratio			Citation
				Immuno-blotting	Immuno-precipitation	Immuno-fluorescence	
Mouse monoclonal	PTEN	A2B1	Santa Cruz (sc-7974)	1:1000		1:200	(Zhang *et al*, 2016)
Rabbit monoclonal	PTEN	138G6	Cell Signaling (#9559)	1:1000			(Wan & Helman, 2003)
Rabbit polyclonal	AKT		Cell Signaling (#9272)	1:1000			(Franke *et al*, 1997)
Rabbit polyclonal	AKT Phospho (S473)		Cell Signaling (#9271)	1:1000			(Franke *et al.*, 1997)
Rabbit polyclonal	β-actin		MBL (pm053)	1:5000			(Wang *et al*, 2015)
Mouse monoclonal	GAPDH	1C4	Sungene Biotech (KM9002)	1:5000			N/A
Mouse monoclonal	FLAG	M2	Sigma-Aldrich (F3165)	1:5000	1:500	1:300	(Gu *et al*, 2016)
Mouse monoclonal	β-tubulin	3G7	Sungene Biotech (KM9003)	1:5000			N/A
Mouse polyclonal	PTENα		Homemade		1:500		(Liang *et al*, 2014)
Rabbit polyclonal	eIF2A		Proteintech (11233-1-AP)	1:1000			(Kim *et al*, 2011)

Rabbit polyclonal	eIF5		Abcam (ab153730)	1:2000			N/A
Rabbit polyclonal	E-cadherin		Proteintech (20874-1-AP)	1:3000			(Zhu *et al*, 2012)
Rabbit polyclonal	β-catenin		Cell Signaling (#9562)			1:200	(Adorno *et al*, 2018)
Mouse monoclonal	FSCN1	OTI3D2	ORIGENE (TA807295)	1:500			N/A
Rabbit polyclonal	CDC42		Cell Signaling (#2462)	1:1000			(Corona *et al*, 2018)
Rabbit polyclonal	VASP		Abcam (ab205952)	1:1000			(Zhan *et al*, 2018)
Rabbit polyclonal	ACTR2		Sigma-Aldrich (A1232)	1:1000			(Ilatovskaya *et al*, 2013)
Rabbit polyclonal	ACTR2 Phospho (T237/T238)		Abcam (ab119766)	1:1000			(Miller *et al*, 2018)
Rabbit polyclonal	VASP Phospho (S157)		Cell Signaling (#3111)	1:1000			(Srihirun *et al*, 2018)
Rabbit polyclonal	VASP Phospho (S239)		Cell Signaling (#3114)	1:1000			(Ruppert *et al*, 2018)
Rabbit polyclonal	VASP Phospho (T278)		Sigma-Aldrich (SAB4200521)	1:1000			(Lawrence & Pryzwansky, 2001)

Mouse monoclonal	ACTR2	E-12	Santa Cruz (sc-166103)			1:100	(Zhao *et al*, 2020)
Mouse monoclonal	CDC42	B-8	Santa Cruz (sc-8401)			1:100	(Oprea *et al*, 2015)
Rabbit monoclonal	VASP	9A2	Cell Signaling Technology (#3132)			1:200	(Cho *et al*, 2016)
Mouse monoclonal	FSCN1	55K-2	Santa Cruz (sc-21743)			1:50	(Megiorni *et al*, 2005)
Mouse monoclonal	His	OTI2B5	ZSGB-BIO(TA-02)	1:1000			NA

Appendix Table S2. Primers for constructing plasmids

Vector	Forward primer (5'-3')	Backward primer (5'-3')
PTEN-GFP	CCGGAATTGCCACCATGCATGACAGCCATCATCAAAGAG	CGCGGATCCGCGACTTTTGTAATTTGTGTATGC
PTENα-GFP	CCGGAATTGCCACCATGCCTGGAGCGGGGGGGAGAAG	CGCGGATCCGCGACTTTTGTAATTTGTGTATGC
PTENβ-GFP	CCGGAATTGCCACCATGCATTTCCAGGGCTGGGAACG	CGCGGATCCGCGACTTTTGTAATTTGTGTATGC
PTENε-GFP	CCGGAATTGCCACCATGGCTGCTGAGGAGAAGCAGG	CGCGGATCCGCGACTTTTGTAATTTGTGTATGC
PTEN-S-tag	CCGGAATTGCCACCATGCATGACAGCCATCATCAAAGAG	CGCGGATCCGACTTTTGTAATTTGTGTATGC
PTENα-S-tag	CCGGAATTGCCACCATGCCTGGAGCGGGGGGGAGAAG	CGCGGATCCGACTTTTGTAATTTGTGTATGC
PTENβ-S-tag	CCGGAATTGCCACCATGCATTTCCAGGGCTGGGAACG	CGCGGATCCGACTTTTGTAATTTGTGTATGC
PTENε-S-Tag	CCGGAATTGCCACCATGGCTGCTGAGGAGAAGCAGG	CGCGGATCCGACTTTTGTAATTTGTGTATGC
PTENα-His	CCGGAATTCCTGGAGCGGGGGGGAGAAG	CGCGGATCCGACTTTTGTAATTTGTGTATGC

FLAG-FSCN1	GATAAGAGCCCGGGCGGATCCACCGC CAACGGCACAGCCG	GATAAGCTTGATATCGAATTCCTAGTA CTCCCAGAGCGAG
FLAG-CDC42	GATAAGAGCCCGGGCGGATCCCAGA CAATTAAGTGTGTTG	GATAAGCTTGATATCGAATTCTCATAG CAGCACACACCTG
FLAG-VASP	GATAAGAGCCCGGGCGGATCCAGCG AGACGGTCATCTGTTC	GATAAGCTTGATATCGAATTCTCAGGG AGAACCCCGCTTC
FLAG-ACTR2	GATAAGAGCCCGGGCGGATCCGACA GCCAGGGCAGGAAGG	GATAAGCTTGATATCGAATTCTTATCG AACAGTCACACCAAG

Appendix Table S3. Primers for mutagenesis

Vector	Forward primer (5'-3')	Backward primer (5'-3')
PTENα CTG^{513}>CTC	CGGCACCTCCCGCTCCTCGAGC GGGGGGGAGAAG	CTTCTCCCCCCCGCTCGAGGAGC GGGAGGTGCCG
PTENα ATT^{594}>CTC	GAGTCGCCTGTCACCCTCTCCA GGGCTGGGAAC	GTTCCCAGCCCTGGAGAGGGTGA CAGGCGACTC
PTENα ATG^{1032}>ATA	CACAGGCTCCCAGACATAACAG CCATCATCAAAG	CTTTGATGATGGCTGTTATGTCTG GGAGCCTGTG
PTENα TCT^{783}>TAG	GAGGATTATTCGTCTTAGCCCC ATTCCGCTGCC	GGCAGCGGAATGGGGCTAAGAC GAATAATCCTC
PTENα AGA^{942}>TAG	GCTACCGCCAAGTCCTAGGCCA TTTCCATCCTG	CAGGATGGAAATGGCCTAGGACT TGGCGGTAGC
PTENα AGG^{810}>CTC	GCTGCCGCCGCTGCCCTCCCTCT GGCTGCTGAG	CTCAGCAGCCAGAGGGAGGGCA GCGGCGGCAGC
PTENα CTG^{816}>CTC	GCCGCTGCCAGGCCTCTCGCTG CTGAGGAGAAG	CTTCTCCTCAGCAGCGAGAGGCC TGGCAGCGGC
PTENα AAG^{831}>CTC	CTGGCTGCTGAGGAGCTCCAGG CCCAGTCGCTG	CAGCGACTGGGCCTGGAGCTCCT CAGCAGCCAG
PTENα CTG^{846}>CTC	AAGCAGGCCCAGTCGCTCCAAC CATCCAGCAGC	GCTGCTGGATGGTTGGAGCGACT GGGCCTGCTT
PTENα CTG^{936}>CTC	GCATCAGCTACCGCCCTCTCCA GAGCCATTTCC	GGAAATGGCTCTGGAGAGGGCGG TAGCTGATGC
PTENε CTG^{816} downstream palindrome disruption	ACAAGCCCAGTCGCTACAACCA TCCAGCAGCCGCCGCAGC	GTTGTAGCGACTGGGCTTGTTTCT CCTCAGCAGCCAGAGG
PTENε 28AA-34AA delete	GCGGTCCAGGGGGCATCAGCTA CCGCC	TGATGCCCCCTGGACCGCAGCCG GGTAATG
PTENε 38AA-50AA delete	GGGGCATCAAAGCCCCGCCACC AGCAGC	GCGGGGCTTTGATGCCCCTCGCT CTGCC

PTENε 57AA-66AA delete	CACCAGCAGAGCCACAGGCTCCCAGACATG	CCTGTGGCTCTGCTGGTGGCGGGGCTTC
PTENε 69AA-81AA delete	TTCAGCCACAGCAGAAACAAAAGGAGATATC	GTTTCTGCTGTGGCTGAAGAAAAAGGAG
PTENε Y210L	GTAATGATATGTGCATTATTATTACATCGGGGC	GCCCCGATGTAATAATAATGCACATATCATTAC

Appendix Table S4. Primers for real-time PCR

Targets	**Forward primer (5'-3')**	**Backward primer (5'-3')**
PTEN(Human)	ATTGCAGAGTTGCACAATATCC	AATAATACACATAGCGCCTCTG
eIF2A(Human)	GCAAGTTGATGACCAGAAATC	GCAATATCAGAAGTGATAAGG
eIF5(Human)	TCAGCTTATCTCCAAGATTCCA	AATACACCACCTCAATGTTCTC
ACTB(Human)	ACAATGAGCTGCGTGTGGCTC	CTGGGGTGTTGAAGGTCTCAAAC

References

Adorno M, di Robilant BN, Sikandar SS, Acosta VH, Antony J, Heller CH, Clarke MF (2018) Usp16 modulates Wnt signaling in primary tissues through Cdkn2a regulation. *Sci Rep* 8: 17506

Cho KJ, Casteel DE, Prakash P, Tan L, van der Hoeven D, Salim AA, Kim C, Capon RJ, Lacey E, Cunha SR *et al* (2016) AMPK and Endothelial Nitric Oxide Synthase Signaling Regulates K-Ras Plasma Membrane Interactions via Cyclic GMP-Dependent Protein Kinase 2. *Mol Cell Biol* 36: 3086-3099

Corona C, Pasini S, Liu J, Amar F, Greene LA, Shelanski ML (2018) Activating Transcription Factor 4 (ATF4) Regulates Neuronal Activity by Controlling GABABR Trafficking. *J Neurosci* 38: 6102-6113

Franke TF, Kaplan DR, Cantley LC (1997) PI3K: downstream AKTion blocks apoptosis. *Cell* 88: 435-437

Gu X, Mao X, Lussier MP, Hutchison MA, Zhou L, Hamra FK, Roche KW, Lu W (2016) GSG1L suppresses AMPA receptor-mediated synaptic transmission and uniquely modulates AMPA receptor kinetics in hippocampal neurons. *Nat Commun* 7: 10873

Ilatovskaya DV, Chubinskiy-Nadezhdin V, Pavlov TS, Shuyskiy LS, Tomilin V, Palygin O, Staruschenko A, Negulyaev YA (2013) Arp2/3 complex inhibitors adversely affect actin cytoskeleton remodeling in the cultured murine kidney collecting duct M-1 cells. *Cell Tissue Res* 354: 783-792

Kim JH, Park SM, Park JH, Keum SJ, Jang SK (2011) eIF2A mediates translation of hepatitis C viral mRNA under stress conditions. *EMBO J* 30: 2454-2464

Lawrence DW, Pryzwansky KB (2001) The vasodilator-stimulated phosphoprotein is regulated by

cyclic GMP-dependent protein kinase during neutrophil spreading. *J Immunol* 166: 5550-5556

Liang H, He S, Yang J, Jia X, Wang P, Chen X, Zhang Z, Zou X, McNutt MA, Shen WH *et al* (2014) PTENalpha, a PTEN isoform translated through alternative initiation, regulates mitochondrial function and energy metabolism. *Cell Metab* 19: 836-848

Megiorni F, Indovina P, Mora B, Mazzilli MC (2005) Minor expression of fascin-1 gene (FSCN1) in NTera2 cells depleted of CREB-binding protein. *Neurosci Lett* 381: 169-174

Miller HE, Larson CL, Heinzen RA (2018) Actin polymerization in the endosomal pathway, but not on the Coxiella-containing vacuole, is essential for pathogen growth. *PLoS Pathog* 14: e1007005

Oprea TI, Sklar LA, Agola JO, Guo Y, Silberberg M, Roxby J, Vestling A, Romero E, Surviladze Z, Murray-Krezan C *et al* (2015) Novel Activities of Select NSAID R-Enantiomers against Rac1 and Cdc42 GTPases. *PLoS One* 10: e0142182

Ruppert M, Korkmaz-Icoz S, Li S, Brlecic P, Nemeth BT, Olah A, Horvath EM, Veres G, Pleger S, Grabe N *et al* (2018) Comparison of the Reverse-Remodeling Effect of Pharmacological Soluble Guanylate Cyclase Activation With Pressure Unloading in Pathological Myocardial Left Ventricular Hypertrophy. *Front Physiol* 9: 1869

Srihirun S, Piknova B, Sibmooh N, Schechter AN (2018) Phosphorylated vasodilator-stimulated phosphoprotein (P-VASPSer239) in platelets is increased by nitrite and partially deoxygenated erythrocytes. *PLoS One* 13: e0193747

Wan X, Helman LJ (2003) Levels of PTEN protein modulate Akt phosphorylation on serine 473, but not on threonine 308, in IGF-II-overexpressing rhabdomyosarcomas cells. *Oncogene* 22: 8205-8211

Wang G, Li Y, Wang P, Liang H, Cui M, Zhu M, Guo L, Su Q, Sun Y, McNutt MA *et al* (2015) PTEN regulates RPA1 and protects DNA replication forks. *Cell Res* 25: 1189-1204

Zhan R, Wang F, Wu Y, Wang Y, Qian W, Liu M, Liu T, He W, Ren H, Luo G (2018) Nitric oxide induces epidermal stem cell de-adhesion by targeting integrin beta1 and Talin via the cGMP signalling pathway. *Nitric Oxide* 78: 1-10

Zhang H, Zhou X, Xu C, Yang J, Xiang J, Tao M, Xie Y (2016) Synergistic tumor suppression by adenovirus-mediated ING4/PTEN double gene therapy for gastric cancer. *Cancer Gene Ther* 23: 13-23

Zhao K, Wang D, Zhao X, Wang C, Gao Y, Liu K, Wang F, Wu X, Wang X, Sun L *et al* (2020) WDR63 inhibits Arp2/3-dependent actin polymerization and mediates the function of p53 in suppressing metastasis. *EMBO Rep* 21: e49269

Zhu L, Qin H, Li PY, Xu SN, Pang HF, Zhao HZ, Li DM, Zhao Q (2012) Response gene to complement-32 enhances metastatic phenotype by mediating transforming growth factor beta-induced epithelial-mesenchymal transition in human pancreatic cancer cell line BxPC-3. *J Exp Clin Cancer Res* 31: 29